Multi-cell three phase AC-DC driver for HB-LED lighting applications

Ignacio Castro, *Student Member, IEEE*, Diego G. Lamar, *Member, IEEE, Manuel Arias, Member, IEEE, Marta M. Hernando, Senior Member, IEEE and Javier Sebastian, Senior Member, IEEE.*

***Abstract*—High Brightness Light-Emitting Diodes (HB-LEDs) are becoming omnipresent across all aspects of illumination products, due to their incredible characteristics: efficiency, reliability, long lifetime, controllability, etc. This paper proposes power conversion topologies to drive medium to high power HB-LEDs in three phase power grids when these connection is available. For that reason, an evaluation of several drivers for medium to high power HB-LEDs in three-phase power grids is done. Moreover, a new topology is proposed which complies with IEC 1000-3-2 Class C requirements, achieves high Power Factor (PF), low Total Harmonic Distortion (THD), as well as, the capability to have a flicker free behaviour while disposing of the bulk capacitor and having galvanic isolation. The HB-LED driver is based on a modular approach with several cells working together with their inputs connected to the three-phase network and their outputs connected in parallel generating a dc output. Each one of these cells is a DC-DC converter operating as a Loss Free Resistor (LFR). In order to validate the concept a prototype has been built by the use of flyback converters operating in Discontinuous Conduction Mode (DCM). Furthermore, it operates in the full range of the European three-phase line voltage, which varies between 380V and 420V, and it supplies an output voltage of 48V with maximum power of 90 W.**

***Index Terms*— Three-phase, AC-DC power conversion, Power Factor Correction, HB-LED driver, Loss Free Resistor.**

I. INTRODUCTION

High-Brightness Light-Emitting Diodes (HB-LEDs) are becoming increasingly ubiquitous across all aspects of illumination products, by offering a lot of advantages over traditional lighting solutions. Some of these advantages will allow LED light sources to have improved functionalities and be more than just a lightbulb (i.e. data transmission, light color, hue and intensity control, people detection, etc.). That is why HB-LEDs are prone to replace traditional lights in household, commercial and industrial installations for a wide variety of power ranges from 50W to 10kW (i.e. medium power bulbs, tunnel lights, stadium spotlights, floodlights, etc.). Furthermore, several of these commercial and industrial installations around the globe receive primary three-phase power with a wide variety of voltages depending on the country, e.g. line-neutral is 347V in Canada, 480V in the US [1] or 230V in the European Union with the exception of the UK (240V). Hence, one question arises, why is not a specific solution for HB-LEDs used when a three phase connection is available.

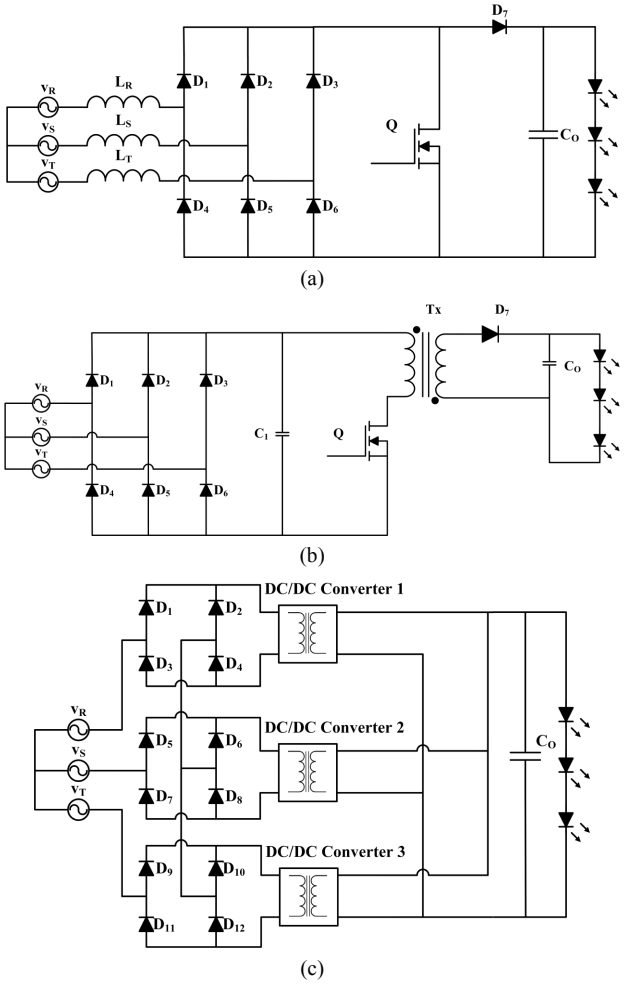

Fig. 1. Evaluation of topologies for driving HB-LEDs. (a) Boost operating in DCM [10]. (b) DC-DC flyback connected to a three phase full wave rectifier. (c) Three phase rectifier based on using three single phase converters with fictional neutral connection [18].

This work has been supported by the Spanish Government under Project MINECO-13-DPI2013-47176-C2-2-R, the Principality of Asturias under the "Severo Ochoa" grant BP14-140 and the Project FC-15-GRUPIN14-143 and by the European Regional Development Fund (ERDF) grants.

HB-LED drivers are normally designed for single-phase universal input voltage supplies (80 to 270V). Therefore, the use of these HB-LED drivers in installations with exclusive access to three-phase normally requires a step-down autotransformer, as well as, access to neutral due to the high voltages in some locations [2]. The use of a step-down autotransformer reduces the efficiency of the whole system greatly due to their electrical efficiency not being higher than ~95%. However, the most important aspect that needs to be taken into account is the size and weight increase of the power supply when a step-down autotransformer is used [3]. Furthermore, one of the main advantages of a three phase driver for HB-LEDs over a single phase driver is the complete removal of the traditional electrolytic capacitor present in single phase AC-DC converters, since the power is not pulsating in a balanced three phase power grid [4]. This fact is key to increase both the lifetime and the light quality of the driver, since an electrolytic capacitor suffers from low life expectancy at high temperatures of roughly 10,000h which compared to the HB-LEDs 100,000h becomes a liability. Hence, the necessity of a compact solution specifically designed for three phase power grids.

In order to design the driver the harmonic injection regulation IEC 1000-3-2 [5]-[7] is going to be followed. It should be classified into Class A taking into account that it is balanced three-phase equipment. Nevertheless, taken into account the fact that it is also lighting equipment, if the driver was single-phase AC-DC it would be classified into Class C. Therefore, the aim of this work will be for the HB-LED driver to comply with the more restrictive of the two, which is Class C, to guarantee low harmonic injection.

In prior literature, several works have been dedicated to the study of AC-DC three-phase switching power supplies [8]. A driver for HB-LEDs is required to be as compact, light and cheap as possible, meaning that a boost converter, see Fig. 1 (a), working either in Discontinuous Conduction Mode (DCM) or Pseudo-Boundary Conduction Mode (PBCM) can be a plausible solution [9], [10]. However, the output voltage required to comply with Class C will be extremely high in this solution to have both high Power Factor (PF) and low Total Harmonic Distortion (THD). There are solutions based on passive filtering the input current in order to obtain a sinusoidal current waveform to be able to comply with the regulation and lower the output voltage, but they will increase the size and weight of the driver dramatically [11]. It should also be noted, that with the DCM boost solution the HB-LEDs will be connected to a high voltage bus [12], and even if this solution is acceptable it might not comply with safety regulation in some cases due to the lack of galvanic isolation. Another possibility without galvanic isolation would be to use a switched capacitor converter [13].

For the sake of lowering the output voltage and compliance with safety regulations, galvanic isolation will be considered mandatory. In that sense, the most popular driver for LEDs are based on the flyback converter from the buck-boost family. However, if a flyback is connected directly to a three-phase power grid, see Fig. 1 (b), the input currents in each phase will not be sinusoidal since the conduction angle for each phase will be $\pi/3$, therefore not complying with Class C from IEC 1000-3-2.

In order to obtain high quality sinusoidal input waveforms, several three-phase buck-boost have been proposed based on a single switch [14], [15] or even two switches [16] to lower the voltage strain on them. However, these topologies require the use of a transformer with three windings, whose coupling will dictate the quality of the input current.

The other option under evaluation for driving LEDs is depicted in Fig. 1 (c) based on a multi-cell converter, that was proposed by Delco as a three phase rectifier using thyristors as the main switches, but it has never been proposed for LED driving [17]. This approach is based on having three single phase converters in a star or delta connection to the three phase power grid and a parallel connection at the output. In that sense, it might be possible to use a three-phase converter based on several cells working as Loss Free Resistor (LFR) as an HB-LED driver [18].

These converters based on a modular approach are more complex from a control point of view since they add more components and are arguably more expensive, but they have a better trade-off between output voltage and THD. Moreover, the design of each module is equivalent to that of a single-phase converter. Several works have been dedicated to the study of these converters, based on DC/DC converters used as cells such as, DCM flybacks [18]-[20], Ćuk [21], SEPIC [22], used as LFR cells. This work proposes the use of this type of multi-cell three phase rectifier as an HB-LED driver considering their advantages over the other topologies expounded.

It should be noted, that some work has been previously done in the field of three-phase dimmable lighting, in the case of fluorescent lamps [23].

Therefore, this paper contributes with two compact, modular, fully dimmable, three-phase AC-DC HB-LED drivers with galvanic isolation. One of them based on a well-known three-phase AC-DC configuration (Delco topology), which is shown in Fig. 1 (c). The second one is the proposed topology [20] [24] of this paper, by means of using LFR cells as can be seen in Fig. 2, which will be extensively described in Section II. Section III will be dedicated to the dynamic analysis of the proposed HB-LED driver and the control circuit which is common for both drivers. Section IV will synthesize the most relevant experimental results for the two drivers that this paper proposes and a comparison will be made between the two by using a Flyback converter as the LFR cell to do the proof of concept of the topology. Finally, the conclusions of this work will be discussed.

In summary, this paper proposes two compact, modular, fully dimmable, three-phase AC-DC HB-LED drivers instead of single-phase ones making it possible to remove the most critical device from the point of view of the converter lifespan, which is the electrolytic capacitor while guaranteeing a flicker free behaviour. The price to pay is to connect the LED driver to a 3-wire line, which is not always available, instead of a 2-wire one with a single phase driver that normally requires the electrolytic capacitor due to the pulsating power. Therefore, the aim of this

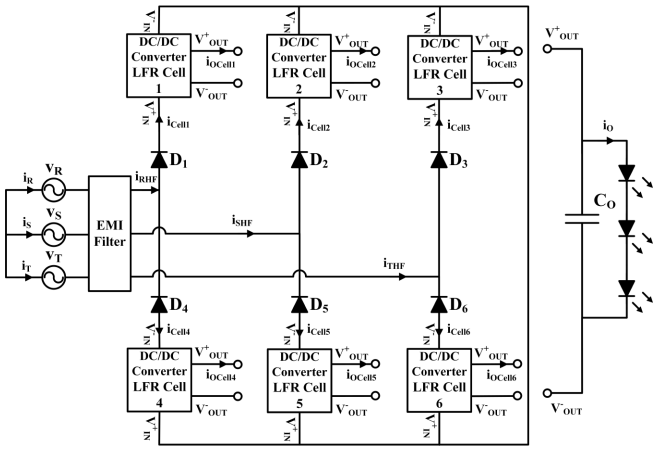

Fig. 2. Diagram of the proposed multi-cell three-phase HB-LED driver [19].

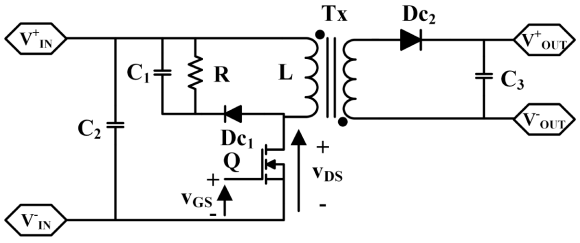

Fig. 3. Schematic of the LFR flyback cell.

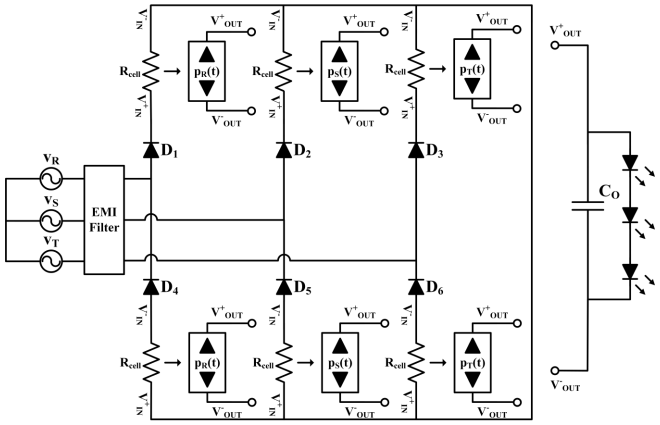

Fig. 4. Simplified diagram of the proposed three phase HB-LED driver with input resistors and power sources for each dc-dc converter.

work is not to change the AC power distribution, but to use the three phase connection to directly drive the HB-LED where it is accessible with a modular, compact and isolation solution.

II. Proposed LED Driver

The concept of the HB-LED driver proposed in this work is based on connecting three single phase AC-DC converters, each of them handling a phase, connected to the three phase power grid by using a star, see Fig. 1 (c), or delta connection, with their outputs connected in parallel. In these three phase power supplies the connection to the neutral is optional. Furthermore, they obtain high quality current at the input of each phase, as

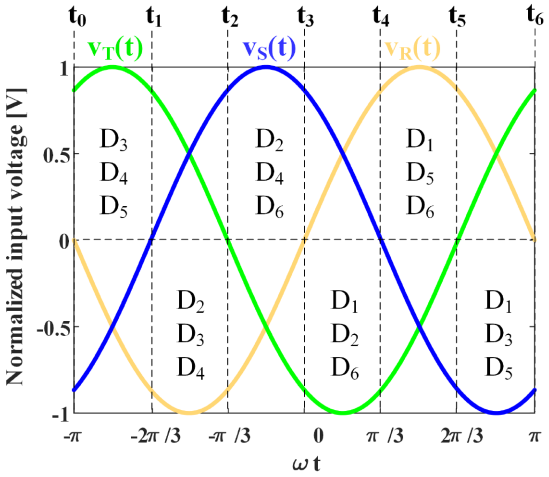

Fig. 5. Theoretical conduction of the diodes depending on the phase voltages.

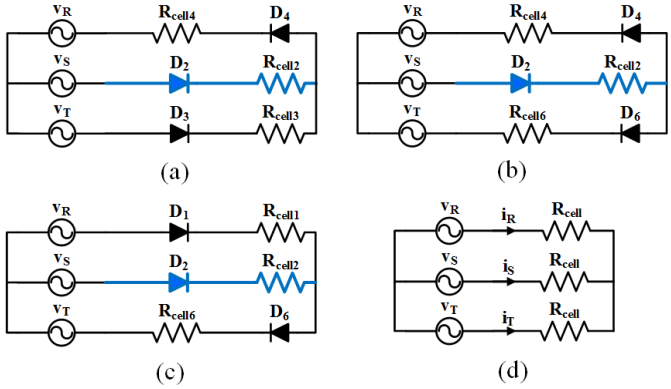

Fig. 6. (a) Conduction during [t_1, t_2] (b) Conduction during [t_2, t_3] (c) Conduction during [t_3, t_4] (d) Simplified working behaviour of the driver.

long as, each AC-DC converter composing the three phase power supply behaves as a resistor from the input [19].

The proposed HB-LED driver is depicted in Fig. 2 [20], where each one of the cells is a LFR. In said figure, V_{IN}^+ and V_{IN}^- represent the input ports of each cell and V_{OUT}^+ and V_{OUT}^- the output ports which are connected to the LEDs. The proposed cells in order to validate the concept of this work are going to be flyback converters working in Discontinuous Conduction Mode (DCM), as depicted in Fig. 3 and whose ports correspond with those of Fig. 2. However, any dc-dc converter able to operate as a LFR is suitable to be used as a LFR cell, as it has been previously explained in [20]. In fact, other LFR cells will be able to achieve better efficiency than the flyback based one.

As has been stated in [25], a flyback working in DCM supplies a fixed amount of current to the load, which in this case are HB-LED. The LFR value of a DCM flyback converter, which is the basic cell of the proposed three phase HB-LED driver, can be defined by:

$$R_{cell} = \frac{2L}{d^2 T}, \qquad (1)$$

where d is the duty cycle of the converter, L is the magnetizing inductance of the transformer referred to the primary side and T is the switching period. By forcing the flybacks to work in DCM with a fixed duty cycle, it can be assured that each one of the flybacks behaves as a resistor at

their input. Hence, each phase will demand a sinusoidal current granting both high PF and low THD.

Henceforth, to simplify the analysis of the HB-LED driver, in Fig. 4 the LFR cells are going to be considered as ideal resistors and the output as an ideal power source, where p_R, p_S and p_T represent the power of each phase. The value of the resistors is going to be considered equal (R_{cell}) not taking into account tolerances that could come from the components of the flyback.

In order for the HB-LED driver to demand a theoretical sinusoidal current, each one of the diodes needs to be conducting during half line cycle. The upper diode of each phase (i.e. D_1, D_2 and D_3) is going to conduct during the positive half line cycle of the phase voltage, whereas, the lower diode (D_4, D_5 and D_6) is going to conduct during the negative half line cycle. Moreover, there are two diodes dedicated per each phase: D_1 and D_4 are dedicated to v_R, D_2 and D_5 are dedicated to v_s and D_3 and D_6 are dedicated to v_T. Hence, three different diodes are going to be conducting every $\pi/3$ of ωt, depending on the phase voltages (v_R, v_S, v_T), as it is summarized in Fig. 5. This is an advantage of the proposed topology when compared with the Delco topology [19], where the line currents undergo the voltage drop corresponding to six rectifier diodes. However, a double amount of converters is required for the proposed topology.

For instance, D_2 is the upper diode of phase S. Hence it will conduct during the positive half line cycle of phase S (i.e. from t_1 to t_4), as stated in Fig. 5. During this time, there are two other diodes conducting. However, they do not share the exact same conduction time as D_2 (i.e. [t_1, t_4]) as they are in charge of rectifying the other two phases R and T. Hence, D_3 swaps with D_6 when phase T goes from positive to negative and D_4 swaps with D_1 when phase R goes from negative to positive.

Therefore, the driver can be divided in three stages for each one of the diodes. These three stages are depicted as an example for diode D_2 in Fig. 6 (a), (b) and (c), where D_2 is the diode that conducts from t_1 to t_4 and D_1, D_3, D_4 and D_6 are the diodes that are swapping in between depending on the voltages of phases R and T.

The analysis done for D_2 is equivalent for the rest of the diodes. Hence, if the whole line period where to be considered, the HB-LED driver is equivalent to a star connection, as shown in Fig. 6 (d), meaning that the input current of each phase (i_N) of the converter is going to be defined by,

$$i_N = \frac{v_N(t)}{R_{cell}} = \frac{v_p}{R_{cell}}\cos(\omega t - \varphi_N), \qquad (2)$$

where v_N is the phase-neutral voltage of one of the phases (N defines whether is phase R, S or T), v_p is the peak amplitude of the phase-neutral voltage and φ_N is the phase of the signal.

Assuring unity PF does not allow to have pulsating power at the HB-LED driver input when considering the power of the three phases. Therefore, the input power of the converter can be defined by the sum of the input power in each phase,

$$p(t) = \sum_{i=1}^{3} \frac{v_N^2(t)}{R_{cell}} = \frac{3v_p^2}{2R_{cell}} = P_g\,, \qquad (3)$$

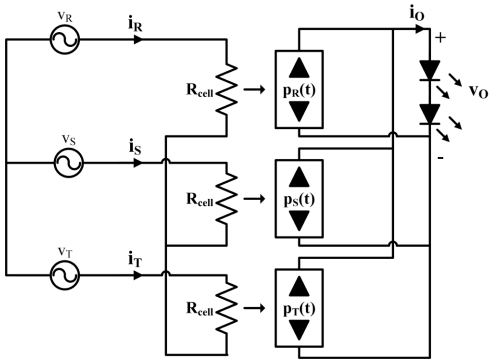

Fig. 7. Three-phase HB-LED driver simplified with LFR.

where it is considered that the input current of each phase follows the input phase voltage ideally.

It should be noted, that the sinusoidal components that come out from the summation in (3) can be removed due to their sum being equal to zero. Hence, the input power of the converter can be defined by a DC component. By combining (1) and (3), the next expression can be yield,

$$P_g = \frac{3v_p^2 d^2 T}{4L}. \qquad (4)$$

Regarding the connection of the outputs, every single secondary side of the LFR cells is going to be connected in parallel to the HB-LEDs (i.e. V_{OUT}^+ and V_{OUT}^-, see Fig. 3). Accordingly, if the simplification from Fig. 6 (d) is taken into account with the parallel output connection, Fig. 7 can be derived. In this figure the basic operation of the converter is explained with the three active cells that are feeding the HB-LED string, keeping in mind the cell behaviour as a power source, which is exactly the same situation as the one in the Delco topology.

The parallel output connection allows the complete removal of the bulk capacitor due to the non-pulsated power given to the HB-LEDs. Hence, a film capacitor can be used to reduce the switching frequency ripple and diminish the low frequency ripple that can still appear due to non-idealities. Furthermore, being able to eliminate the bulk capacitor from the HB-LED driver, increases dramatically the lifespan of the driver. Particularly important for lighting environments with either difficult access or expensive solutions that need to guarantee a high lifespan of the driver.

Therefore, if non-pulsated power is given to the HB-LEDs. A relation can be made between input power (3) and output power (P_O), yielding,

$$P_g = \frac{3v_p^2}{2R_{cell}} = i_o v_o \rightarrow M = \frac{v_o}{v_p} = \sqrt{\frac{3}{2R_{cell} i_o}}\,, \qquad (5)$$

where i_O is the current through the LEDs and v_O is the output voltage the HB-LEDs withstand.

From solving (1) into (5), the duty cycle required to drive the switches of the HB-LED driver can be obtained,

$$d = \frac{2}{v_p}\sqrt{\frac{L i_o v_o}{3T}}, \qquad (6)$$

considering that the same PWM signal is going to be driving all the flyback converters.

Full dimming on the HB-LEDs is achieved by reducing the duty cycle, which increases the emulated resistance diminishing the output current while keeping theoretical sinusoidal input current. From the design point of view, both the theoretical duty cycle (5) and the maximum output power (3) need to be calculated for the required specifications of the designer. It needs to be kept into consideration that the nominal duty cycle for the three phase driver is going to be smaller than the theoretical duty calculated for a single phase flyback [25]. This is extremely important in order to optimize the cells of the driver. Afterwards, the LFR flyback cell needs to be designed, as has been explained previously in [19], considering an input voltage in the cells equal to the one of the phase-neutral. Furthermore, the designer needs to keep in mind that, each flyback is going to be handling one sixth of the input power, this is important in order to design the cell thermally considering that is going to be more relaxed than in the classic topology. However, in terms of semiconductors the cell needs to be rated for one third of the power of the driver, since the cells are working during half line cycle for each phase.

III. Control Strategies

Closed loop operation is mandatory in most applications where a certain voltage or current level needs to be guaranteed at the output. HB-LED drivers are no exception especially considering that changes can occur on the load due to temperatures changes or ageing. Moreover, a certain voltage/current level needs to be assured in order to guarantee not only good light quality, but to avoid harmful effects for human beings in commercial and industrial environments.

From the schematic depicted in Fig. 7, the control of the HB-LED driver can be synthesized as a problem of three power supplies connected in parallel to the same load. Many works in previous literature have addressed the parallelization of powers supplies [26]-[28]. From these works a quick conclusion can be extracted: the most optimal way to control the power supplies (LFR cells), would be for each one of them to have their own input current loop in order for them to demand the same amount of power. However, in the case under study that means the use of a current sensor for each cell, which leads to six current sensors. This solution would increase not only the price but the complexity of the control.

It is important to note that the tolerances of the components are going to have an effect over the LFR value (R_{cell}). Especially the tolerance of L which is the most critical component in this sense. This variation of the R_{cell} from one cell to another will have an effect on the output voltage and current of the driver in terms of a 100 Hz component, as the power processed by each cell will differ causing input power slightly to pulsate. Therefore, an independent current control for each cell would be optimal to reduce the tolerance effects or any unbalance that could come from the three-phase grid [29]. However, since the change between R_{cell} is extremely small, it does not justify the use of a more complex control, as will be seen in Section IV. Hence, an output current loop like the one depicted in Fig. 8 is going to be used.

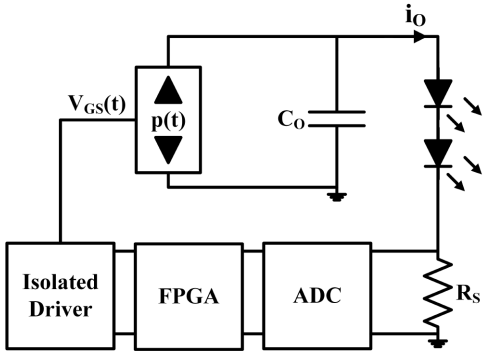

Fig. 8. HB-LED driver current loop diagram.

The current loop proposed in Fig. 8, is going to be based on measuring the output current by means of a shunt resistor. The sensed voltage, which is proportional to the current through the HB-LEDs, is going to be digitally converted and processed by an FPGA, in order to generate the digital pulse-width modulation (DPWM) that goes to the isolated driver of each cell. The signal that goes into each isolated driver is V_{GS} (t), meaning that the main switch of each cell is going to be driven by the same signal.

In order to determine the compensator to be used in the HB-LED driver, the transfer function of the HB-LED driver needs to be calculated using an equivalent analysis to the one done in [19] by using the average small signal analysis, presented in [30] for single phase AC-DC converters. Consequently, the starting point for this analysis would be the input power handled by the HB-LED driver, defined by (3), and the equation that can be obtained from the circuit in Fig. 8, which is defined in (7),

$$p(t) = C_O v_o(t) \frac{dv_o(t)}{dt} + v_o(t) i_o(t), \tag{7}$$

where v_o can be defined by,

$$v_o(t) = i_o(t) r_{LED} + V_{rLED}, \tag{8}$$

where r_{LED} is the equivalent dynamic resistance and V_{rLED} is the equivalent knee voltage of the HB-LED strings. Note that, V_{rLED} is a constant value that will be removed from the dynamic analysis due to its non-dynamic variation. Hence, the HB-LED string can be modelled by r_{LED}.

By equating (3) and (7), equation (9) can be derived. Note that both v_p and d are dependent on time. The first one due to the variations that can occur in a three-phase grid considering that voltage changes occur at the same time in the three phases in order to simplify the analysis. And the second one due to the duty cycle variation required to regulate the output voltage.

$$\frac{3v_p^2(t)}{2R_{cell}(t)} - C_O i_o(t) r_{LED}^2 \frac{di_o(t)}{dt} - i_o^2(t) r_{LED} = 0 \tag{9}$$

After perturbing equation (9), particularizing for the flyback by substituting (1) and eliminating the second order and the DC terms, equation (10) can be reached. Note that lower case letters have been used for the static analysis and capital letter will be used for constant values and to particularize the equation in a determined point of operation.

TABLE I
COMPONENTS OF THE EXPERIMENTAL LFR CELL PROTOTYPE

Fig. 4 reference	VALUE
Dc_1	STTH208U
Dc_2	FES8BT-E3/45
C_1	1 µF 800 V Ceramic Cap.
C_2	100 nF 50 V Film Cap.
C_3	1 µF 50 V Film Cap.
R	10.5 kΩ
Q	IPP65R225C7
Tx	Coilcraft Z9007-BL

TABLE II
REST OF COMPONENTS OF THE HB-LED DRIVER

Fig. 2 reference	VALUE
D_1-D_6	1N4007
C_O	10 µF 100 V Film Cap.
FPGA	XC7A100T-1CSG324C

$$\frac{3V_p^2DT}{2L}\hat{d} + \frac{3V_pD^2T}{2L}\hat{v}_p - C_o r_{LED}^2 I_o \frac{d\hat{\imath}_o}{dt} - 2I_o r_{LED}\hat{\imath}_o = 0 \quad (10)$$

From (10), it is immediate to obtain the relationships between i_o and d, and i_o and v_p required to control the HB-LED driver. Hence, (11) and (12) are obtained by applying the Laplace transformation to (10) and equating the corresponding terms,

$$G_{i_o d}(s) = \left.\frac{\hat{\imath}_o(s)}{\hat{d}(s)}\right|_{\hat{v}_p=0} = \sqrt{\frac{3T}{4Lr_{LED}}}\frac{V_P}{\left(\frac{C_O r_{LED} s}{2}+1\right)} \quad (11)$$

$$G_{i_o v_p}(s) = \left.\frac{\hat{\imath}_o(s)}{\hat{v}_p(s)}\right|_{\hat{d}=0} = \frac{I_o}{V_P\left(\frac{C_O r_{LED} s}{2}+1\right)} \quad (12)$$

It is important to note that the implementation has been done by means of a digital control. Therefore, limit cycling needs to be taken into account in the design of the compensator, in this case by using the definitions that guarantee non limit cycling performance in PFC [31]. However, it is possible to obtain similar results with the use of an analog control.

The designer needs to keep in mind that the regulator needs a crossover frequency of less than 300 Hz to guarantee that there is no frequency component having an effect over the control action. These effects can appear in the output due to two non-idealities not considered in the theoretical analysis. Firstly, as it was previously explained the tolerances of the components that comprise the LFR cells. And secondly, the quality of the input voltage that can suffer variations during its operation causing a 300 Hz component to appear, as it will be shown in Section IV when a real connection to the three phase power grid is used. The lower crossover frequency decreases the bandwidth of the system, causing the driver to have a slower response. However, HB-LEDs are a very stable load and the slower response is not problematic. This is the reason why a more costly and complex control system has not being studied to reduce this effect.

Another fact that is extremely important to take into account when closing the loop, is that the driver gains the ability to vary the duty cycle, therefore having the ability to change the value

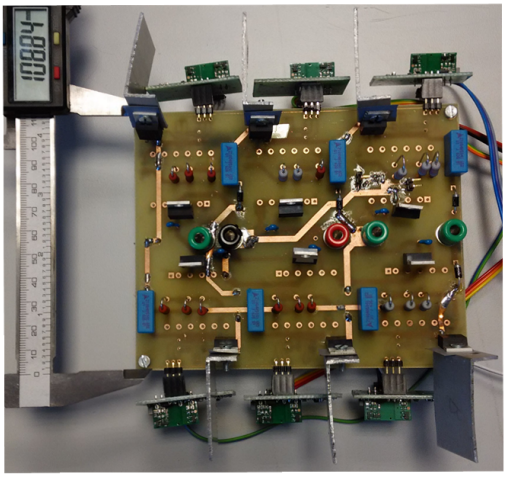

(a)

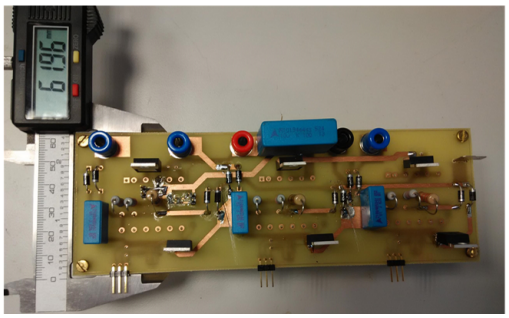

(b)

Fig. 9. HB-LED driver prototypes with measurements done in millimeters. (a) Proposed LED driver. (b) Classic topology.

of the R_{cell}. This means that R_{cell} varies with ωt, which implies that there can exist some input current distortion that will have an impact on the PF and the THD. So if rapid changes are allowed the unity factor correction can be compromised causing the output voltage and current to increase their ripple. Designing a low crossover frequency as mentioned before is enough of a solution to this problem, as was reported in [24].

Finally, the start-up procedure of the converter for the flyback LFR cells, will consist in slowly increasing the duty cycle from 0% until it reaches the required output current stated by the control. This procedure can be explained with (1), by carefully increasing the duty cycle of the cell, the LFR values will decrease, therefore, giving more power to the HB-LEDs. In the case of other LFR cells the start-up procedure might differ [33].

IV. EXPERIMENTAL VALIDATION

A. *Description and basic results.*

This paper proposes the HB-LED driver introduced in Section II and the Delco [17] topology shown in Fig. 1 (c) for driving HB-LEDs. Both topologies have been designed for a maximum power of 90W using the same components for the flyback cells to be able to compare both topologies. These drivers receive a three-phase input of 400Vrms line-to-line and feeding in the process five strings of 12 HB-LED (W42180T2-SW) with their respective equalizing resistor. This load is equivalent to 1.8A/48V at full load. The LFR cell is based on a flyback converter working in DCM at a 100 kHz, as the one

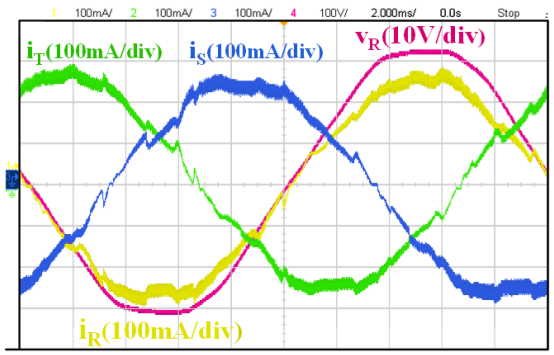

Fig. 10. Input currents for all three phases and input voltage of phase R when the proposed HB-LED driver is fully loaded.

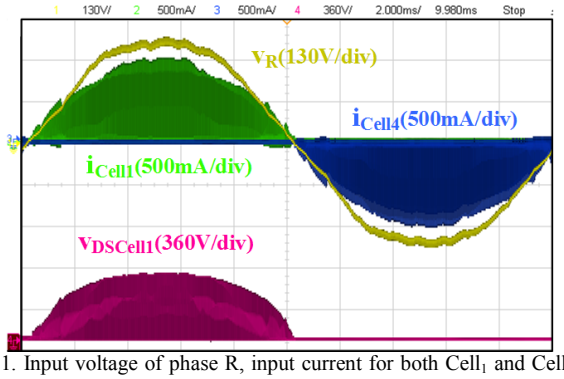

Fig. 11. Input voltage of phase R, input current for both $Cell_1$ and $Cell_4$ and drain-source voltage for $Cell_1$.

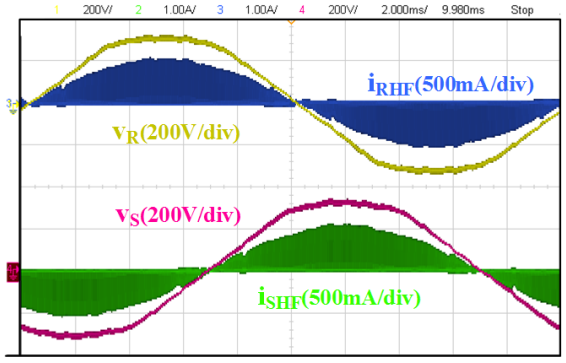

(a)

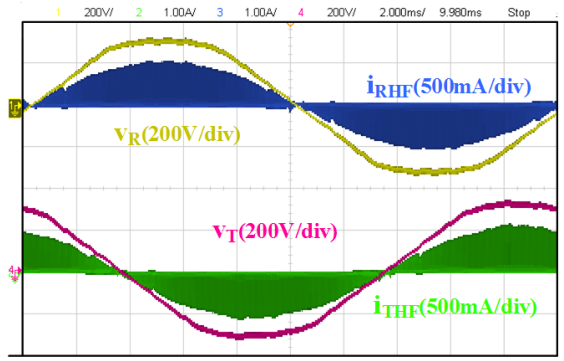

(b)

Fig. 12. Input voltage and high frequency input current (a) Phases R and S. (b) Phases R and T.

shown in Fig. 3, whose components are summarized in Table I. The LFR behaviour of the flyback cell has been validated at switching frequency by means of a Venable® 6320 Frequency Response Analyzer (FRA) [32]. Furthermore, each one of these flyback converters handles one sixth of the total power as it was previously stated for the proposed converter and one third in the case of the Delco topology, meaning that each one handles 15W in the case of the proposed driver and 30W in the other. The rest of the components that comprise the HB-LED drivers are summarized in Table II. Fig. 9 shows a picture of both prototypes, which were built to validate the concept of this work. It should be noted that the flyback coupled inductors are on the bottom side of the board. The testing effectuated in this section has been done with both prototypes connected to the real three-phase power grids, with the same string of HB-LEDs connected to the output of both drivers and with the same flyback cell.

This connection to the real three-phase power grid, is what justifies the distortion of V_R in Fig. 10. This figure shows a snapshot of the oscilloscope for the proposed HB-LED driver where the input currents of the driver, as well as, one of the phase-neutral input voltages of the converter can be observed. As can be seen, the current (i_R) follows the voltage (v_R) demonstrating that power factor correction is achieved for the proposed driver. The phase shift between currents is $2\pi/3$ of ωt, so it can be assumed that power correction in the three phases is achieved. However, these measurements show the filtered currents before the EMI filter. In order to correctly exemplify the operation of the cells dedicated to an specific branch, Fig. 11, shows the input currents for the two LFR cells dedicated to phase R ($cell_1$ and $cell_4$), relating to the currents specified in Fig. 2. As it can be observed, $cell_1$ works during the positive half line cycle of phase R, whereas $cell_4$ works during the negative half line cycle. Therefore, assuring the correct operation of both cells in the proposed topology. The same is supposed true for the other two phases which are not shown. Please note that in the Delco topology the cell works during both positive and negative half line cycle. Fig. 11, also shows the voltage between drain and source that the main switch of cell1 withstands.

Fig. 12 (a) and (b), show the high frequency currents measured after the EMI filter, see Fig. 2, that the proposed HB-LED driver demands from the grid with its respective phase voltages. These figures show that the cells follow correctly its input voltage and the current that each cell is demanding. Phase R is shown in both figures as a reference to correctly exemplify the phase shift between phase voltages (i.e. v_R, v_S and v_T).

As it was previously introduced, the cell consists on a flyback converter working as a LFR by operating in DCM. Fig. 13 (a), shows the experimental operation of one of the cells, in this case particularized for $cell_1$, being its behaviour equivalent for the rest of the cells that comprise the proposed topology. As it can be seen, the cell only operates during half line cycle and it only supplies energy to the load during this period, see I_{OCell1}. In order to show that the cell is correctly operating in DCM, two zooms of Fig. 13 (a) are taken and shown in both Fig. 13 (b) and Fig. 13 (c), the first zoom is taken nearby the peak of the phase voltage (i.e. 310V) and the second at 200V. These figures, show that the cell is operating at constant frequency to achieve the required DCM, in order to work as a LFR, and that the cut off of the drain to source voltage is correctly done at 600V by the action of a clamping snubber to prevent the destruction of the MOSFETs.

Furthermore, the proposed HB-LED driver needs to feed the HB-LEDs with a constant voltage/current. Hence, the output

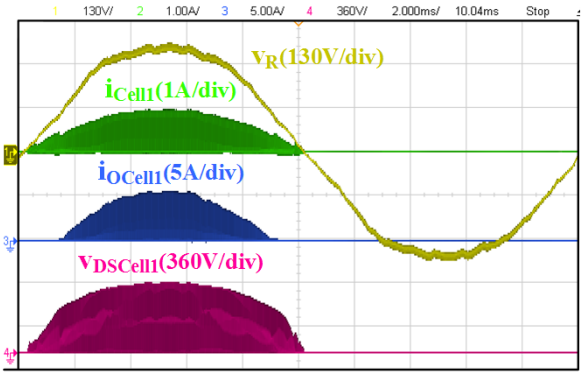

(a)

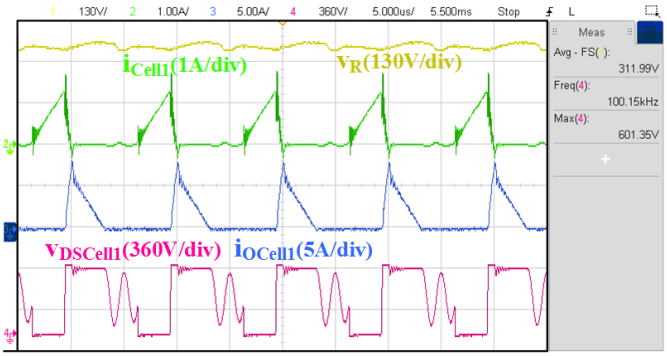

(b)

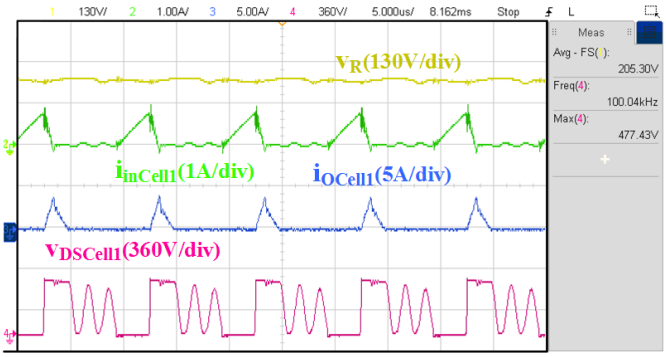

(c)

Fig. 13. Operation of cell$_1$ of the proposed converter. (a) Mains frequency operation (b) Zoom near the peak value of the phase voltage (i.e. 310V). (c) Zoom at 200V.

voltage of the HB-LED driver is measured and shown in Fig. 14. In order to validate the concept of the proposed driver the high frequency output currents are also measured and shown in said figure. The currents are measured by conjoining the high frequency output currents of the six cells in groups of two related to the current each branch is demanding (i.e. $i_{OR} = i_{Cell1}+i_{Cell4}$, $i_{OS} = i_{Cell2}+i_{Cell5}$, $i_{OT} = i_{Cell3}+i_{Cell6}$). As can be observed, i_{OR}, i_{OS} and i_{OT} are extremely similar, meaning that the output power provided by each cell will also be similar. Accordingly, by summing i_{OR}, i_{OS} and i_{OT}, the high frequency output current of the driver can be obtained. This current is filtered by the output capacitor obtaining the output current that it is fed to the HB-LED string, i_O, which can be seen in Fig. 15. Although, in Fig. 15, it can be observed that both the low frequency output current and the output voltage have low ripple with a 10µF film capacitor for the proposed driver, a 300 Hz ripple appears in both the output current and voltage. This 300 Hz component comes from the fact that the input voltage is not

TABLE III
SUMMARY OF THD AND PF FOR THREE DIFFERENT OUTPUT CURRENTS IN THE PROPOSED LED DRIVER

Output Current/Phase		1.8A	0.9A	0.45A
R	PF[%]	99.81	99.72	99.56
	THD[%]	5.71	6.97	8.03
S	PF[%]	99.87	99.75	99.59
	THD[%]	4.62	6.96	7.71
T	PF[%]	99.85	99.73	99.58
	THD[%]	5.26	6.86	7.97

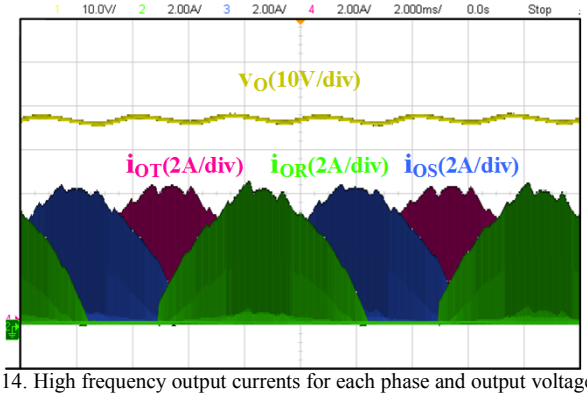

Fig. 14. High frequency output currents for each phase and output voltage for the proposed HB-LED driver when fully loaded.

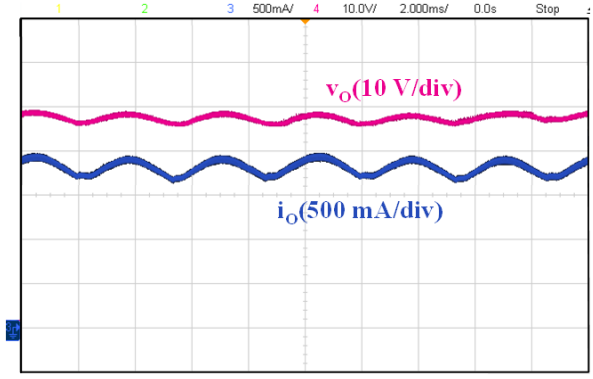

Fig. 15. Output current and output voltage for the proposed HB-LED driver when fully loaded.

a pure sinusoidal waveform in fact it seems cropped near the peak of the sinusoid, as it can be seen in Fig. 10. Hence, the input power is not constant against what was derived in (3), meaning that some degree of variation should occur at the load in terms of voltage and current, as can be seen in Fig. 14 output currents.

In order to validate both HB-LED drivers, several measurements are going to be taken into account. Firstly, to validate the dimming of the HB-LED driver, three operating points are going to be measured by varying the voltage reference of the loop, therefore, varying the output current to 1.8A (fully loaded), 0.9 A and 0.45 A.

To correctly analyze the waveforms in both scenarios, they are going to be extracted from the oscilloscope as data and processed with MATLAB®. The parameters that are going to be extracted for each one of the points are: efficiency, THD, PF, compliance with Class C IEC 1000-3-2 [5]-[7] for both, and flicker operating recommendation [34], [35] for the dimming validation.

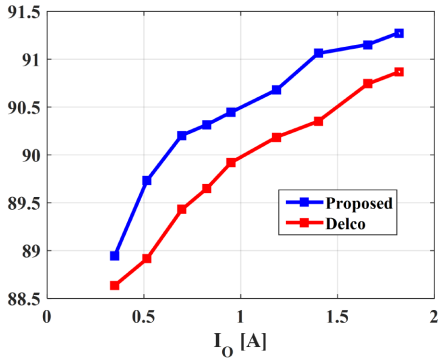

Fig. 16. Efficiency versus output current for both prototypes, not taking driving losses into account.

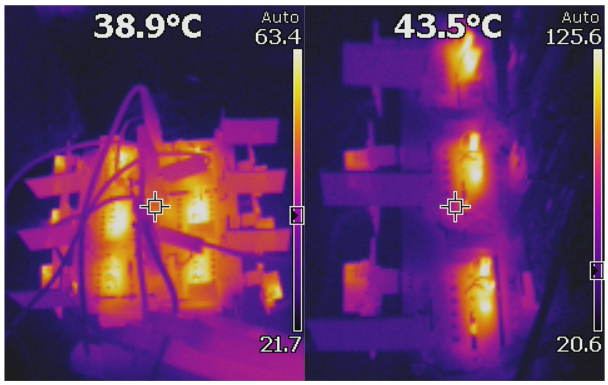

(a) (b)

Fig. 17. Thermal behaviour of two topologies under study. (a) Proposed. (b) Delco.

B. Dimming validation of the HB-LED driver.

The dimming validation is shown for the proposed driver in Table III, which summarizes PF and THD measurements for each phase based on the input voltages and input currents extracted from the oscilloscope for the three operating points stated before. As can be seen, high PF and low THD is achieved even in dimming conditions. The efficiency of the proposed HB-LED driver is compared with the Delco topology showing a slightly better performance in Fig. 16, without taking into account driving losses, which are around 1.5W for both prototypes. These difference in efficiency between the two solutions are explained due to two fact previously introduced in Section II. The first being the amount of diodes conducting in each topology and the second related to the conduction time of the converters. In the Delco topology the converters will be working all the time whereas in the proposed topology they will be working every 20ms. This difference, will lead to a difference in temperature, as is shown in Fig. 17, where the Delco topology presents its maximum temperature at a value almost doubling that of the proposed topology.

It can be seen that the efficiency decreases by lowering the output current, being roughly 88% at the full dimming point. It should be noted that the efficiency of the driver was not the aim of this work, since it was proving the concept of feeding HB-LED in three-phase power grids and testing the concept of the proposed topology.

The waveforms have also been used to extract the harmonics by using the Fourier series on them. Afterwards, these measurements are compared with Class C IEC 1000-3-2 harmonic limits. As can be seen in Fig. 18, both drivers comply with Class C, and their input current harmonics are quite similar, as expected.

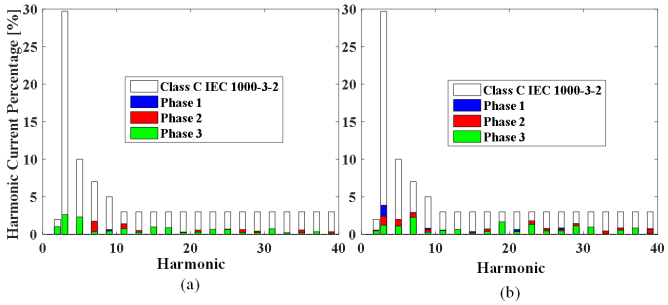

Fig. 18. Harmonic content of each phase for both topologies under study and compliance with Class C. (a) Proposed. (b) Delco.

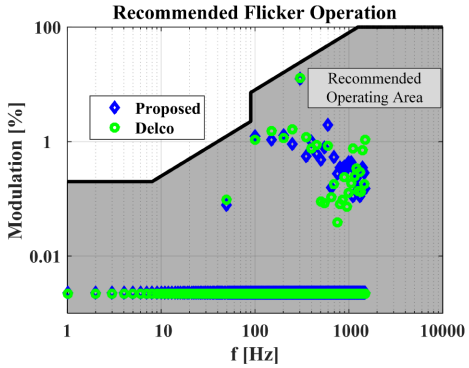

Fig. 19. Recommended flicker operation at full load for both drivers, P1789 [35].

To limit the biological effects and detection of flicker in general illumination, the Modulation (%) should be kept within the shaded region defined in [34], [35], where the Modulation(%) calculation can be define as follows:

$$Modulation\ (\%) = 100 \cdot \frac{(L_{max} - L_{min})}{(L_{max} + L_{min})}, \qquad (13)$$

where L_{max} and L_{min} correspond to the maximum and minimum luminance of each harmonic of the AC component of the output current, respectively.

The luminance of the HB-LEDs have been measured for both drivers, being the waveforms for all the points under study extremely similar. After obtaining the luminance waveforms, all the harmonics have been obtained from 1 Hz to 3 kHz and compared with the graph proposed in the standard, as can be seen Fig. 19. As can be seen, all the harmonic content for both drivers falls within the shaded region, even the ones below 90Hz which are the most crucial. Therefore, good light quality and non-harmful effects can be assumed from the HB-LED drivers presented.

V. CONCLUSIONS

Two three-phase fully dimmable HB-LED drivers with galvanic isolation based on a multi-cell structure have been reported and experimentally validated in this work. The original topology proposed in this work has been compared with the Delco topology which is commonly used in three phase power grids and closely related to the proposed topology due to its

modularity. This comparison has been made by using a flyback converter as a LFR cell in order to make the proof of concept due to its simplicity to achieve a LFR behaviour.

The efficiency study showed a slight improvement of performance for the proposed topology over the Delco topology due to the two advantages introduced in the previous sections: the lower number of low frequency diodes conducting at the same time and the fact that the converters work only during positive or negative half line cycle, therefore lowering the overall temperature of the system. However, these advantages come at the cost of almost doubling the amount of components. Hence, the proposed driver is suitable and might be justifiable in terms of cost for really high power spotlights up to 10 kW as it scales better than the Delco topology.

In the case of high power spotlights, it should be considered the use of more suitable LFR cells, as a flyback converter would be a limiting factor due to its low efficiency and high input current ripple due to its operation in DCM. The aim of this work was not to propose the flyback for the whole range of operation but rather do a proof of concept of the proposed topology by using a converter that was able to achieve a LFR behaviour in a simplistic manner. In fact, the flyback cell would only be recommended for operation under several hundred watts (up to 500W) in the case of the proposed topology. Therefore, taking into account the limitations of the DCM flyback, the higher power scenarios can be tackled in two ways, either by using a LFR cell based on a two stage solution with a boost PFC with a multiplier based control followed by an isolated dc-dc converter or with the parallelization or/and serialization of more cells [20]. The proposal of this work is driving LEDs in three phase grids with the Delco topology from 50 W to 2 kW, and use the proposed driver for the range from 2 kW to 10kW.

Furthermore, the proposed HB-LED driver has been experimentally validated, obtaining significant advantages over a single phase connection, since both HB-LED drivers built in this work dispose of the electrolytic capacitor traditionally present in PFC, while complying with both the flicker and the harmonic injection regulation. Hence, the HB-LED drivers introduced in this work are proposed for stadiums, industrial or commercial environments, where high power spotlights are required and three-phase grids are available.

REFERENCES

[1] ANSI C84.1 – 2011, American National Standard for Electric Power Systems and Equipment – Voltage Ratings (60 Hz).

[2] Gray, B. "Demystifying 347V and 480V Lighting Installations. " [online] E Craftsmen.

Available at: http://www.ecraftsmen.com/blog/demystifying-347v-and-480v-lighting-installations [Accessed 20 Oct. 2015].

[3] GE lighting, "480V to 277V Step-Down Autotransformers For applications up to 375 Watts", 2013.

[4] M. Arias, A. Vazquez, and J. Sebasti ´ an, “An overview of the AC-DC ´ and DC-DC converters for LED lighting applications,” Automatika—J. Control, Measure., Electr., Comput. Commun., vol. 53, pp. 156–172, 2012

[5] Draft of the Proposed CLC Common Modification to IEC 61000-3-2 Document, 2006.

[6] Draft of the Proposed CLC Common Modification to IEC 61000-3-2/A2 Document, 2010.

[7] Electromagnetic Compatibility (EMC)-Part 3: Limits-Section 2: Limits for Harmonic Current Emissions (Equipment Input current < 16 A per Phase), IEC1000-3-2, 1995.

[8] B. Singh, B. N. Singh, A. Chandra, K. Al-Haddad, A. Pandey and D. P. Kothari, "A review of three-phase improved power quality AC-DC converters," in IEEE Transactions on Industrial Electronics, vol. 51, no. 3, pp. 641-660, June 2004.

[9] A. R. Prasad, P. D. Ziogas and S. Manias, "An active power factor correction technique for three-phase diode rectifiers," Power Electronics Specialists Conference, 1989. PESC '89 Record., 20th Annual IEEE, Milwaukee, WI, 1989, pp. 58-66 vol.1.

[10] D. S. L. Simonetti, J. Sebastian and J. Uceda, "Single-switch three-phase power factor preregulator under variable switching frequency and discontinuous input current," Power Electronics Specialists Conference, 1993. PESC '93 Record., 24th Annual IEEE, Seattle, WA, 1993, pp. 657-662.

[11] Y. Jang and M. M. Jovanovic, "A novel, robust, harmonic injection method for single-switch, three-phase, discontinuous-conduction-mode boost rectifiers," Power Electronics Specialists Conference, 1997. PESC '97 Record., 28th Annual IEEE, St. Louis, MO, 1997, pp. 469-475 vol.1.

[12] C. S. Wong, K. H. Loo, Y. M. Lai, M. H. L. Chow and C. K. Tse, "An Alternative Approach to LED Driver Design Based on High-Voltage Driving," in IEEE Transactions on Power Electronics, vol. 31, no. 3, pp. 2465-2475, March 2016.

[13] R. Coutinho; K. Souza; F. Antunes; E. Sa, "Three-Phase Resonant Switched Capacitor LED Driver with Low Flicker," in IEEE Transactions on Industrial Electronics , vol.PP, no.99, pp.1-1.

[14] M. R. Mendonça, E. Mineiro; Sá, R. P. Coutinho and F. L. M. Antunes, "AC-DC single-switch three-phase converter with peak current control for power LEDs," Industry Applications (INDUSCON), 2014 11th IEEE/IAS International Conference on, Juiz de Fora, 2014, pp. 1-6.

[15] J. W. Kolar, H. Ertl and F. C. Zach, "A novel three-phase single-switch discontinuous-mode AC-DC buck-boost converter with high-quality input current waveforms and isolated output," in IEEE Transactions on Power Electronics, vol. 9, no. 2, pp. 160-172, Mar 1994.

[16] F. Stogerer, J. Minibock and J. W. Kolar, "Design and experimental verification of a novel 1.2 kW 480VAC /24VDC two-switch three-phase DCM flyback-type unity power factor rectifier," Power Electronics Specialists Conference, 2001. PESC. 2001 IEEE 32nd Annual, Vancouver, BC, 2001, pp. 914-919 vol.2.

[17] R. F. Brewster and A. H. Barret, “Three Phase AC to DC voltage converter with Power Line Harmonic Current Reduction”, U.S. patent 4 143 414, March 6, 1979.

[18] M. J. Kocher and R. L. Steigerwald, "An AC-to-DC Converter with High Quality Input Waveforms," in IEEE Transactions on Industry Applications, vol. IA-19, no. 4, pp. 586-599, July 1983.

[19] S. Singer and A. Fuchs, "Multiphase AC-DC conversion by means of loss-free resistive networks," in IEE Proceedings - Circuits, Devices and Systems, vol. 143, no. 4, pp. 233-240, Aug 1996.

[20] J. Sebastian, I. Castro, D. G. Lamar, A. Vazquez and K. Martin, "High power factor modular polyphase AC/DC converters with galvanic isolation based on Resistor Emulators," 2016 IEEE Applied Power Electronics Conference and Exposition (APEC), Long Beach, CA, 2016, pp. 25-32.

[21] U. Kamnarn and V. Chunkag, "Analysis and Design of a Modular Three-Phase AC-to-DC Converter Using CUK Rectifier Module With Nearly Unity Power Factor and Fast Dynamic Response," in IEEE Transactions on Power Electronics, vol. 24, no. 8, pp. 2000-2012, Aug. 2009.

[22] G. Tibola and I. Barbi, "Isolated Three-Phase High Power Factor Rectifier Based on the SEPIC Converter Operating in Discontinuous Conduction Mode," in IEEE Transactions on Power Electronics, vol. 28, no. 11, pp. 4962-4969, Nov. 2013.

[23] M. Sabahi, S. H. Hosseini, M. B. B. Sharifian, A. Y. Goharrizi and G. B. Gharehpetian, "A Three-Phase Dimmable Lighting System Using a Bidirectional Power Electronic Transformer," in IEEE Transactions on Power Electronics, vol. 24, no. 3, pp. 830-837, March 2009.

[24] I. Castro, D. G. Lamar, M. Arias, J. Sebastián and M. M. Hernando, "Three phase converter with galvanic isolation based on loss-free resistors for HB-LED lighting applications," 2016 IEEE Applied Power Electronics Conference and Exposition (APEC), Long Beach, CA, 2016.

[25] R. Erickson, M. Madigan and S. Singer, "Design of a simple high-power-factor rectifier based on the flyback converter," Applied Power Electronics Conference and Exposition, 1990. APEC '90, Conference Proceedings 1990., Fifth Annual, Los Angeles, CA, USA, 1990, pp. 792-801.

[26] J. S. Glaser and A. F. Witulski, "Application of a constant-output-power converter in multiple-module converter systems," Power Electronics Specialists Conference, 1992. PESC '92 Record., 23rd Annual IEEE, Toledo, 1992, pp. 909-916 vol.2.

[27] Yuehui Huang and C. K. Tse, "Circuit theoretic classification and performance comparison of parallel-connected switching converters," 2008 IEEE International Symposium on Industrial Electronics, Cambridge, 2008, pp. 196-201.

[28] Yuehui Huang and C. K. Tse, "Classification of parallel DC/DC converters part II: Comparisons and experimental verifications," Circuit Theory and Design, 2007. ECCTD 2007. 18th European Conference on, Seville, 2007, pp. 1014-1017.

[29] L. Huber, M. Kumar and M. M. Jovanovic, "Analysis, design, and evaluation of three-phase three-wire isolated ac-dc converter implemented with three single-phase converter modules," 2016 IEEE Applied Power Electronics Conference and Exposition (APEC), Long Beach, CA, 2016, pp. 38-45.

[30] R. Ridley, "Average small-signal analysis of the boost power factor correction circuit," in Proceedings of the Virginia Power Electronics Center Seminar, 1989, pp. 108-120.

[31] B. A. Mather and D. Maksimovic, "Quantization effects and limit cycling in digitally controlled single-phase PFC rectifiers," 2008 IEEE Power Electronics Specialists Conference, Rhodes, 2008, pp. 1297-1303.

[32] D. Venable, "Source-load interactions in multi-unit power systems", Venable Technical Paper #12.

[33] M. Kumar, L. Huber and M. M. Jovanovic, "Startup procedure for three-phase three-wire isolated ac-dc converter implemented with three single-phase converter modules," 2016 IEEE Applied Power Electronics Conference and Exposition (APEC), Long Beach, CA, 2016, pp. 46-53.

[34] IES, "RP-16-10, Nomenclature and Definitions for Illuminating Engineering", Illuminating Engineering Society, 2010.

[35] IEEE Recommended Practices for Modulating Current in High-Brightness LEDs for Mitigating Health Risks to Viewers," in IEEE Std 1789-2015 , vol., no., pp.1-80, June 5 2015.

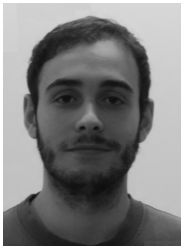

Ignacio Castro (S'14) was born in Gijón, Spain, in 1989.

He received the M.Sc. degree in telecommunication engineering from the University of Oviedo, Gijón, Spain, in 2014, and he is currently pursuing the Ph.D. degree in the same university.

His research interests include low and medium power dc–dc converters, modeling, simulation and control of dc-dc converters and power-factor correction ac–dc converters.

Diego G. Lamar (M'08) was born in Zaragoza, Spain, in 1974. He received the M.Sc. degree, and the Ph.D. degree in Electrical Engineering from the University of Oviedo, Spain, in 2003 and 2008, respectively.

In 2003 and 2005 he became a Research Engineer and an Assistant Professor respectively at the University of Oviedo. Since September 2011, he has been an Associate Professor. His research interests are focused in switching-mode power supplies, converter modelling, and power-factor-correction converters.

Manuel Arias (s'05 M'10) received the M. Sc. degree in electrical engineering from the University of Oviedo, Spain, in 2005 and the Ph. D. degree from the same university in 2010.

In 2007 he joined the University of Oviedo as an Assistant Professor and since 2016 he is an Associate Professor at the same university.

His research interests include ac-dc and dc-dc power converters, battery-cell equalizers and LED lighting.

Marta M. Hernando (M'95-SM'11) was born in Gijón, Spain, in 1964. She received the M.Sc. and Ph.D. degrees in Electrical Engineering from the University of Oviedo, Gijón, Spain, in 1988 and 1992, respectively. She is currently a Professor at the University of Oviedo. Her main interests include switching-mode power supplies and high-power factor rectifiers.

Javier Sebastián (M'87-SM'11) was born in Madrid, Spain, in 1958. He received the M.Sc. degree from the Technical University of Madrid (UPM), and the Ph.D. degree from the University of Oviedo, Spain, in 1981 and 1985, respectively. He was an Assistant Professor and an Associate Professor at both the UPM and the University of Oviedo. Since 1992, he has been with the University of Oviedo, where he is currently a Professor. His research interests are switching-mode power supplies, modeling of dc-to-dc converters, low output voltage dc-to-dc converters, high power factor rectifiers, LED drivers, dc-to-dc converters for envelope tracking techniques and the use of wide band-gap semiconductors in power supplies.